Area Invariance of Apparent Horizons under Arbitrary Lorentz Boosts

Sarp Akcay, Richard A. Matzner, and Vishnu Natchu

University of Texas at Austin *

arXiv:0708.0276v3 [gr-qc] 8 Mar 2009

Abstract

It is a well known analytic result in general relativity that the 2-dimensional area of the apparent horizon of a black hole remains invariant regardless of the motion of the observer, and in fact is independent of the $t = constant$ slice, which can be quite arbitrary in general relativity. Nonetheless the explicit computation of horizon area is often substantially more difficult in some frames (complicated by the coordinate form of the metric), than in other frames. Here we give an explicit demonstration for very restricted metric forms of (Schwarzschild and Kerr) vacuum black holes. In the Kerr-Schild coordinate expression for these spacetimes they have an explicit Lorentz-invariant form. We consider *boosted* versions with the black hole moving through the coordinate system. Since these are stationary black hole spacetimes, the apparent horizons are two dimensional cross sections of their event horizons, so we compute the areas of apparent horizons in the boosted space with (boosted) $t = constant$, and obtain the same result as in the unboosted case. Note that while the invariance of area is generic, we deal only with black holes in the Kerr-Schild form, and consider only one particularly simple change of slicing which amounts to a boost. Even with these restrictions we find that the results illuminate the physics of the horizon as a null surface and provide a useful pedagogical tool. As far as we can determine, this is the first explicit calculation of this type demonstrating the area invariance of horizons. Further, these calculations are directly relevant to transformations that arise in computational representation of moving black holes. We present an application of this result to initial data for boosted black holes.

*Electronic address: akcays@physics.utexas.edu; Electronic address: matzner2@physics.utexas.edu; Electronic address: vishnu@physics.utexas.edu

I. INTRODUCTION

Apparent horizons (AH) were first introduced by Penrose and Hawking [1], [2]. An apparent horizon is defined as the outermost marginally trapped surface on a given (partial) Cauchy slice. It is a topologically spherical 2-dimensional surface on which the expansion of the outgoing null rays orthogonal to the surface is zero [3]. Thus, it is a surface where gravity is so strong that putative outgoing null rays can only "hover" against the gravitational force. Unlike event horizons, which are globally defined as the boundary in spacetime between null geodesics that escape to infinity, and those that fall into the singularity, apparent horizons are local objects, computable at one instant of time, hence much more accessible in numerical simulations. The locations of event and apparent horizons coincide only in stationary spacetimes. In the stationary Kerr spacetime in Boyer-Lindquist coordinates, the horizon is located at radial coordinate $r = r_+ \equiv M + \sqrt{M^2 - a^2}$, where M is the mass of the black hole and a is the spin parameter for the Kerr black hole given by $a \equiv J/M$, with J being the angular momentum of the black hole; for $a = 0$ we have the static Schwarzschild black hole. Here and henceforth, we use Newton's constant $G = 1$, and speed of light $c = 1$.

In this paper we consider only Kerr spacetimes in Kerr-Schild (KS) coordinates as given in Eq. (1) below. This form of the metric contains a "natural" Minkowski background, and hence a natural definition of a Lorentz boost [4]. It is found (cf. [5], [6], [7]) that the apparent horizon of a black hole will appear distorted in these coordinates when boosted; the longitudinal coordinate direction undergoes a Lorentz contraction. However, this is an effect only in coordinates; the point of this paper is an explicit calculation to show that the area of the apparent horizon 2-surface, recomputed in the spatial frame of the boosted observer, remains unchanged, that is: $Area = 4\pi\left(r_+^2 + a^2\right)$ for the Kerr case and $Area = 16\pi M^2$ for the Schwarzschild black hole. This result is of course necessary on general principles.

The invariance of the area depends on the observation that the event horizon of a stationary black hole is a null 3-dimensional submanifold of the spacetime with vanishing expansion. And null surfaces naturally remain null under Lorentz transformations. In fact, the area of any 2-dimensional cross section of the horizon remains invariant under any redefinition of the 3-space $t = constant$ (that is legitimately spacelike). Two cross sections of the event horizon that differ by a redefinition of $t = constant$ slice can be put in a pointwise 1-to-1 correspondence along the null generators of the horizon. These null offsets do not contribute

to the area which is transverse to the null generators. We give a quick derivation of the Schwarzschild situation and then present the most general calculation for these spacetimes, namely, the Kerr black hole boosted along an arbitrary direction.

The Kerr vacuum solution to Einstein's equation can be written in a special form called the Kerr-Schild form of the metric. This form is, in general ([8], [9], [10], [11]),

$$g_{\mu\nu} = \eta_{\mu\nu} + 2Hl_\mu l_\nu \tag{1}$$

where H is a function of spacetime coordinates, $\eta_{\mu\nu}$ is the Minkowski metric of flat spacetime and l^μ is a null vector with respect to both $g_{\mu\nu}$ and $\eta_{\mu\nu}$. Clearly, this is a special form, and the metric of a general spacetime cannot be put in this form. But the Kerr vacuum black hole can be so written. Under a Lorentz boost (a coordinate transformation with the form of a Lorentz transformation on the t, x, y, z coordinates describing the flat space with metric $\eta_{\mu\nu}dx^\mu dx^\nu$), the Kerr-Schild metric will preserve the general form that it has in Eq. (1). We will place overbars on coordinates in the unboosted frame. In section III, we will show the area invariance for a boosted Kerr black hole by performing a coordinate transformation to facilitate boosting the spacetime, followed by another coordinate transformation that simplifies extracting the 2-dimensional metric by restricting to the horizon. With the 2-dimensional metric we straightforwardly compute the horizon area.

The special case of the nonspinning Schwarzschild (i.e. spherical) black hole provides an illuminating guide to the features of the full Kerr case. Eq. (1) for this case is

$$g_{\mu\nu}d\bar{x}^\mu d\bar{x}^\nu = -d\bar{t}^2 + d\bar{x}^2 + d\bar{y}^2 + d\bar{z}^2 + \frac{2M}{\bar{r}}\left(d\bar{t} + d\bar{x} + d\bar{y} + d\bar{z}\right)^2 \tag{2}$$

which, in cylindrical coordinates $(\bar{r}_{||}, \bar{r}_\perp, \bar{\phi}_{cyl})$ can be written as

$$g_{\mu\nu}d\bar{x}^\mu d\bar{x}^\nu = -d\bar{t}^2 + d\bar{r}_{||}^2 + d\bar{x}_\perp^2 + d\bar{y}_\perp^2 + \frac{2M}{\bar{r}}\left(d\bar{t} + \frac{\bar{r}_{||}}{\bar{r}}d\bar{r}_{||} + \frac{\bar{x}_\perp}{\bar{r}}d\bar{x}_\perp + \frac{\bar{y}_\perp}{\bar{r}}d\bar{y}_\perp\right)^2. \tag{3}$$

where $\bar{x}_\perp = \bar{r}_\perp cos\ \bar{\phi}_{cyl}$ and $\bar{y}_\perp = \bar{r}_\perp sin\ \bar{\phi}_{cyl}$. The coordinate system $(\bar{r}_{||}, \bar{r}_\perp, \bar{\phi}_{cyl})$ aligns $\bar{r}_{||}$ with the axis of the cylinder parallel to the boost direction $\vec{\beta}$; $\bar{r}_\perp, \bar{\phi}_{cyl}$ are the polar coordinates of the circular plane orthogonal to the axis of the cylinder (see Fig. (3)). Note that $\bar{x}^2 + \bar{y}^2 + \bar{z}^2 = \bar{r}_{||}^2 + \bar{r}_\perp^2$.

The boosted (unbarred) coordinates are related to the unboosted frame by

$$\begin{aligned} \bar{t} &= \gamma(t - \beta\, r_{||}) \\ \bar{r}_{||} &= \gamma(r_{||} - \beta\, t) \\ \bar{r}_\perp &= r_\perp\ , \quad \bar{\phi}_{cyl} = \phi_{cyl}. \end{aligned} \tag{4}$$

The boost parameter is $\beta \equiv v/c$, and $\gamma = (1-\beta^2)^{-1/2}$; both are defined as usual in the background Minkowski spacetime. The apparent horizon is defined in a given 3-space ($t = constant$) and the horizon area will be independent of t, so we take $t = 0$. The $t = 0$ (boosted) 3-metric is

$$ds^2|_{t=0} = dr_{||}^2 + dx_\perp^2 + dy_\perp^2 + \frac{2M}{\bar{r}^3}(-\bar{r}\gamma\beta dr_{||} + \bar{r}_{||}d\bar{r}_{||} + \bar{x}_\perp d\bar{x}_\perp + \bar{y}_\perp d\bar{y}_\perp)^2 \,. \tag{5}$$

We have strategically kept some terms expressed using unboosted (barred) forms. They can be straightforwardly substituted using Eq. (4). In this form, however, we can easily restrict the metric to the horizon surface, since

$$\bar{r}d\bar{r} = \bar{r}_{||}d\bar{r}_{||} + \bar{x}_\perp d\bar{x}_\perp + \bar{y}_\perp d\bar{y}_\perp = 0 \tag{6}$$

on the horizon where $\bar{r}$ is a constant ($= 2M$). Thus on the horizon:

$$\begin{aligned} ds^2|_{t=0,\,\bar{r}=2M} &= \left[\gamma^{-2}d\bar{r}_{||}^2 + d\bar{x}_\perp^2 + d\bar{y}_\perp^2 + \frac{2M}{\bar{r}}(\beta^2 d\bar{r}_{||}^2)\right]_{\bar{r}=2M} \\ &= (d\bar{r}_{||}^2 + d\bar{x}_\perp^2 + d\bar{y}_\perp^2)|_{\bar{r}=2M} \,. \end{aligned} \tag{7}$$

In Cartesian $(\bar{x}, \bar{y}, \bar{z})$ coordinates this would look like

$$ds^2|_{t=0,\,\bar{r}=2M} = \left(d\bar{x}^2 + d\bar{y}^2 + d\bar{z}^2\right)|_{\bar{r}=2M} \,. \tag{8}$$

This can be put in a more familiar form using spherical coordinates $(\bar{r}, \bar{\theta}, \bar{\phi})$ which now gives

$$ds^2|_{t=0,\,\bar{r}=2M} = (2M)^2\left(d\bar{\theta}^2 + \sin^2\bar{\theta}d\bar{\phi}^2\right) \,. \tag{9}$$

Thus the area of the horizon is $4\pi(2M)^2$ as expected. Importantly, note that Eq. (7) describes the boosted apparent horizon; the simple form (Eq. (8)) that allows immediate evaluation of the surface area is the expression of this area in terms of coordinates appropriate first of all to the unboosted frame. On the horizon the contribution from the time transformation exactly cancels the Lorentz contraction of $\bar{r}_{||}$.

II. NUMERICAL RESULTS

Before looking at the horizon of a boosted spinning black hole, we demonstrate some numerical applications of these concepts, concentrating in this section on only nonspinning black holes. Recent breakthroughs in numerical relativity ([12], [13], [14], [15], [16], [17]) have

enabled the community to investigate various physical scenarios involving interacting black holes. There are many different approaches to numerically evolving the physical system. The use of a particular structure, *puncture initial data* ([18]) has become ubiquitous for numerical codes. Puncture initial data are conformally flat. Solution of the constraint equations (elliptic equations describing a nonlinear generalization of Newtonian gravity) produces a mathematically correct configuration. But if boosted, the puncture is not physically relaxed, so when the solved (mathematcally correct) data are evolved, the black hole emits short wavelength gravitational radiation. Some of this spurious radiation propagates out to infinity and some falls onto the black hole, increasing the horizon mass.

One can instead use *superposed Kerr-Schild* ([19]) initial data. This takes the Kerr-Schild metric for a single black hole and creates a background metric for two black holes by adding a second 'mass term' to the flat background:

$$g_{\mu\nu} = \eta_{\mu\nu} + H_1 l^{(1)}_\mu l^{(1)}_\nu + H_2 l^{(2)}_\mu l^{(2)}_\nu. \tag{10}$$

Here H_1, H_2 are scalar functions that depend on coordinates from the centers of each black hole as well as the black holes' masses and spins. They are identical in form to single black hole terms centered at the locations of the two holes (cf. Eqs. (1), (2), and also Eq. (11) below; there is also a prescription for superposing the momentum associated with this combination, in the initial data). Although Kerr-Schild initial data exactly solve Einstein's equation for a single boosted black hole and thus satisfy the constraint equations, this is not the case for superposed Kerr-Schild, which is only an educated guess. However, by starting out with this initial guess as a conformal background metric (in the same sense that puncture data has a flat conformal background), one can solve the constraint equations, so Kerr-Schild data can be adjusted to become proper initial data. The solution of the elliptic initial data equations modifies the configuration to be an exact (modulo numerical error) description of a gravitational configuration. In practice, unless the black holes are very close together, the correction for superposed Kerr-Schild data is small; less than one percent.

The code being developed at University of Texas Austin is called *openGR* [20]. Among the suite of programs comprising *openGR*, there is a finite element initial data code, which can produce either puncture or superposed Kerr-Schild initial data. The evolution code treats the dynamics of binary black hole systems and the extraction of gravitational waves from the merger of the black holes. The code is a fourth order accurate adaptive mesh

refinement code with sixth order interpolation between coordinate patches.

The total mass/energy of the spacetime is given by the ADM mass M_{ADM} ([28]) computed at spatial infinity (numerically, "near" the grid boundary). The ADM mass corresponds to the apparent Newtonian mass measured at large distances from the sources, measured for instance by observing the period of distant satellites around the central mass. Suppose the individual black hole masses are given by Kerr-Schild mass parameters m_1 and m_2. Then the *background* gives an ADM mass $M_{ADM\ bkgd} = m_1 + m_2$. As noted, solving the constraint equation changes the superposed Kerr-Schild data slightly, so the solved ADM mass closely approximates $M_{ADM} \approx m_1 + m_2$, though it does have some dependence on the parameters of the data, particularly on the separation of the black holes.

Of interest in the design of data is the binding energy E_b of the configuration. We can compute this as the measured ADM mass minus the intrinsic mass of the constituent black holes. The difficulty lies in defining an intrinsic black hole mass. We choose the horizon mass. (For nonspinning black holes, we have $M_H = (A_H/16\pi)^{1/2}$, where A_H is the area of the apparent horizon; *openGR* includes an apparent horizon finder.) Classically the area of the horizon can increase, but we also know that the horizon area is an adiabatic invariant; it is only slightly affected by slow motions. "Slow" means slow compared to the normal frequencies of oscillation of the hole, which are high frequency; the lowest frequency is on the order $f \sim (20M_H)^{-1}$, and most frequencies in binary evolution are lower than this frequency. Hence we are confident that the apparent horizon provides an (almost) constant intrinsic mass. Binding is indicated by $E_b \equiv M_{ADM} - (M_{H1} + M_{H2}) < 0$. If the data describe black holes in motion, then the kinetic energy also contributes (positively) to the total energy. For a boosted black hole the ADM mass acquires a factor γ: $M_{ADM\ 0} \to \gamma M_{ADM\ 0}$ where $M_{ADM\ 0}$ is m, the metric mass parameter in the single hole case. Thus we expect that for a given boost parameter γ, the binding energy may be negative (i.e. bound) if the holes are close together, but positive (unbound) if the data are set with the black holes far apart. Furthermore, for the nonlinear small separation limit (and/or for significant γ) cases, Newtonian arguments become obscure because of the change in metric due to the presence of the second hole, and due to coordinate ambiguities.

We construct an equal mass binary black hole system (nonspinning Schwarzschild black holes) with initial coordinate separation r. The configuration is axisymmetric; the black holes are boosted toward or away from each other with Lorentz boost velocity $\beta \equiv v/c$ (or

instantaneously at rest with $\beta = 0$); the boosts are equal but opposite in the computational frame. The axisymmetry allows extremely high resolution computational simulation. The code is a finite element code, with an adaptive resolution of $1/100\ M_{ADM}$ near the holes and $1\ M_{ADM}$ at the outer boundary. The computational domain is a sphere of radius $256\ M_{ADM}$.

We plot the the negative of binding energy $-E_b$ of the binary in figure 1. Here, we define the binding energy to be $E_b \equiv M_{ADM} - 2M_H$. Since the configuration is axisymmetric, the black holes have the same horizon mass M_H, hence the factor of 2. We display our results in units of the total parameter ADM mass which is normalized to equal 1 ($M_{ADM\ bkgd} = m_1 + m_2 = 0.5 + 0.5 = 1$). Here r is the coordinate separation between the two black holes also given in units of M_{ADM} (e.g. $r = 10$ translates to $r = 10\, G\, M_{ADM}/c^2$). The binding energy scales as $1/r$ at the Newtonian limit; this Newtonian limit is plotted as a red straight line in Fig. 1. Bonning et al. [21] had analytically predicted this Newtonian limit (see that paper for details). Previous computational work by Hawley et al. [22] failed to show the Newtonian limit, because of insufficient domain size to eliminate outer boundary effects. We clearly see that for every rest configuration the binding energy for large separations agrees with the Newtonian prediction ([21]), but there is a deviation to stronger binding for closer coordinate separation. We will have more to say about this in a future paper. The cause for this will be discussed below as it related to the distortion of black holes' horizons near each other. One can in principle use expressions from post-Newtonian theory to give the next order correction to E_b. These terms scale as $((\text{Mass})/r)^2$. We have begun studying these higher order corrections.

It is of interest to understand *how* the binding energy is achieved in the initial data. Fig. 2 is a plot of M_{ADM} and horizon mass M_H versus $1/r$ for boosts of $\beta = 0,\ 0.1,\ 0.5$ represented by the red, green and black curves for M_H , respectively. For the M_{ADM} versus $1/r$ plot, we use a blue solid line, red "$\times$" marks and pink dashed line for $\beta = 0,\ 0.1,\ 0.5$, respectively. Note the confirmation of the analytical expectation above that the ADM mass is essentially constant for the binary pair regardless of the coordinate distance between them. However, although we construct all data with the same parameter values m, we see different constant ADM masses for different $|\beta|$ (motion with the same $|\beta|$ together or apart yields the same ADM mass, constant across the possible separations). This is because the ADM mass scales as $\gamma\ M_{ADM\,0}$ for a boosted black hole. Thus, for example, the ratio of ADM masses between the pink dashed line ($\beta = 0.5$) and the blue line ($\beta = 0$) in Fig. 2 should

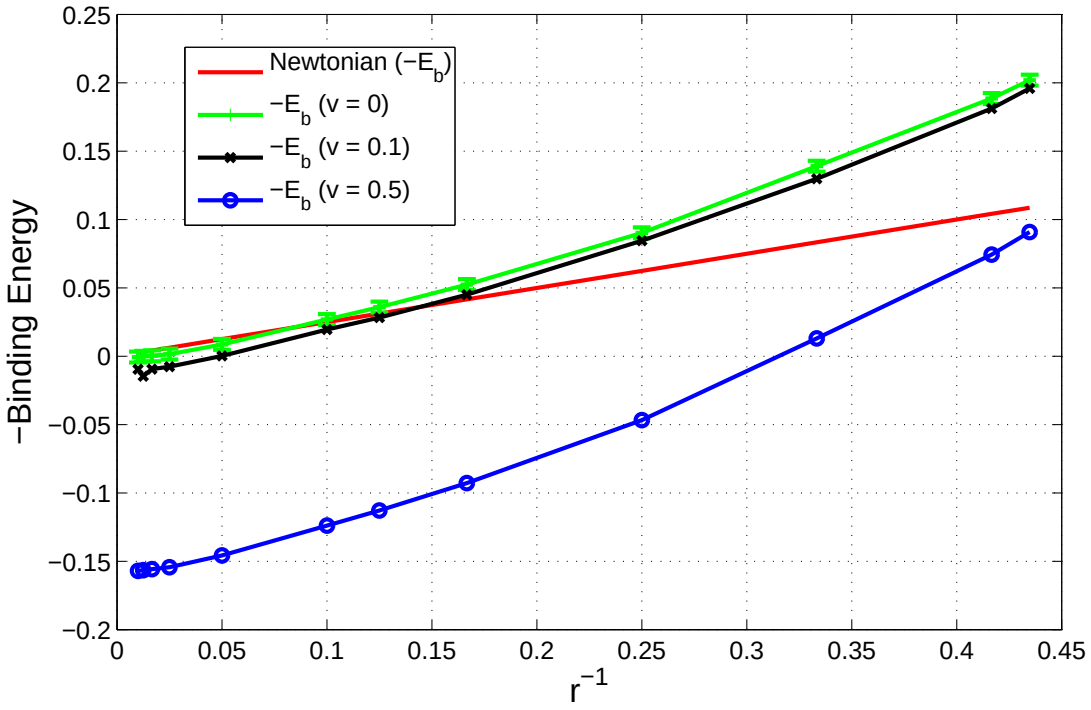


FIG. 1: Negative of the binding Energy $-E_b$ versus the inverse coordinate separation $1/r$ for the cases with boosts speed $\beta = 0,\ 0.1,\ 0.5$ represented by the green, black and blue curves, respectively. The red line is the Newtonian binding energy which scales as $1/r$. Ideally, it should be tangent to the $\beta = 0$ curve (green) at large r ($1/r \to 0$) but here it is slightly shifted due to numerical errors. As can be seen in the figure, the binding energy matches the Newtonian limit very well for large separations ($1/r \to 0$), it grows faster than $1/r$ as the black holes are closer ($1/r \to \infty$). This is due to changes in horizon masses because of the distortions induced by the black holes on each other. It ($-E_b$) also becomes more negative for large boosts reflecting the unbound nature of distant rapidly moving black holes. The kinetic energy of the black holes overwhelms the negative potential energy.

be $(1 - 0.5^2)^{-1/2} = 1.154$. This is easily seen in Fig. 2. We estimate the numerical error of about one percent in this quantity by looking at the ADM mass for the $\beta = 0$ case (blue line) which, in principle, should give $M_{ADM} = 1$ but actually is located slightly higher at $M_{ADM} = 1.01$.

Though M_{ADM} stays almost constant for differing separation, the binding becomes stronger for smaller separation, even in the Newtonian limit, of course. As described in

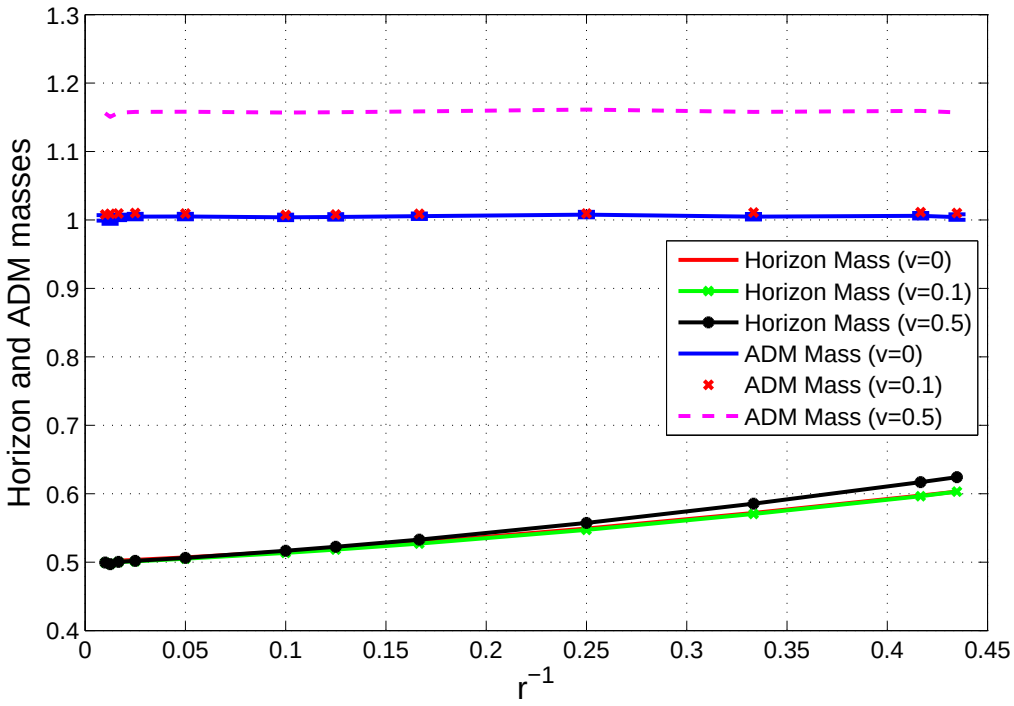


FIG. 2: Horizon mass M_H and ADM mass M_{ADM} versus inverse distance 1/r for boost speeds of $\beta = 0, 0.1, 0.5$. M_{ADM} (the upper, approximately parallel curves) is given by the the pink dashed line (v=0.5) and by the closely overlapping blue line (v=0) and the red tick marks ("×"). As expected, the ADM mass remains constant regardless of the separation r but varies as $\gamma\ M_{ADM\ 0}$ for varying boost speeds β. M_H (the lower curves) is represented by closely overlapping red and green curves for the v=0 and v= 0.1 cases, and by the higher black curve for v= 0.5. Note that the horizon mass grows larger as the black holes are nearer i.e. as $1/r \to \infty$. The horizon mass is invariant under boosts. For $r \geq 10$ (i.e. $1/r \leq 0.1$) the horizon mass curves for different boosts overlap perfectly. Apparently because of the nonlinear interaction of the black hole geometries in the full solution, for larger boosts and for small separations the horizon mass does increase slightly.

[21], when the parameter m is held constant for each hole, the *horizon* area of the constituent black holes increases with decreasing separation. The modification of the geometry by the *other* black hole modifies the horizon area so that it is no longer the $16\pi m^2$ which would be computed for an isolated hole, but $16\pi M_H^2$ with $M_H \neq m$. If we imagine the initial data constructed by adiabatically moving the holes from infinite separation, it would be this mass M_H which is adiabatically invariant. This was predicted analytically by [21]

for nonspinning, instantaneously nonmoving black holes; it was predicted qualitatively for moving black holes.

The horizon mass is expected to remain invariant under boosts, and in single boosted black holes this is what we observe. But for fully solved data – the result of solving a nonlinear elliptic system, Fig. 2 shows that the horizon mass in the $\beta = 0.5$ case is somewhat above that of the $\beta = 0$ one for close separations ('close' meaning black hole separations less than $r = 10$). Indeed, for $r > 10$ (i.e. $1/r < 0.1$), the overlap of the red, green and black curves is perfect to within less than one percent error. This is an interesting result depending on both the boost and the separation. The *growth* of the horizon area for large boosts is an effect due to the proximity of the two black holes. For sufficiently large separations, the boost does not change the horizon mass, hence the horizon area.

III. BOOSTED KERR BLACK HOLE

We return to the analytic study of black hole horizons, now including spin. Strong astrophysical evidence supports the existence of spinning (Kerr) black holes ([23], [24],[25]); manipulating description of this spacetime is a frequent task in computational astrophysics. The angular momentum of the spinning black hole automatically selects a preferred direction and the Kerr hole is axially symmetric around the spin axis. Written in Kerr-Schild coordinates the Kerr spacetime formally admits a boost.

We will begin with the unboosted Kerr metric written in standard Kerr-Schild coordinates. We will then rewrite the metric in cylindrical coordinates where the symmetry axis of the cylinder points toward the boost direction. (We transform to cylindrical coordinates only to facilitate the boosting of the spacetime.) Once the spacetime is boosted, we will look at the spatial 3-metric on a (boosted) $t = constant$ hypersurface. Since we are ultimately interested in the 2-metric we will perform one final coordinate transformation from cylindrical to spheroidal coordinates and consider $\bar{r} = r_+$ (the expected horizon location). Once we have our 2-metric, we will compute the area of the apparent horizon and show that it indeed equals the unboosted, stationary value, which is $Area = 4\pi\left(r_+^2 + a^2\right)$.

The Kerr spacetime in Kerr-Schild coordinates is ([8], [9], [10],[11]):

$$ds^2 = -d\bar{t}^2 + d\bar{x}^2 + d\bar{y}^2 + d\bar{z}^2 + \frac{2M\bar{r}^3}{\bar{r}^4 + a^2\bar{z}^2}\left[d\bar{t} + \frac{\bar{r}\bar{x} + a\bar{y}}{\bar{r}^2 + a^2}d\bar{x} + \frac{\bar{r}\bar{y} - a\bar{x}}{\bar{r}^2 + a^2}d\bar{y} + \frac{\bar{z}}{\bar{r}}d\bar{z}\right]^2$$

$$= -d\bar{t}^2 + d\bar{x}^2 + d\bar{y}^2 + d\bar{z}^2 + \frac{2M\bar{r}^3}{\bar{r}^4 + a^2\bar{z}^2}\left[d\bar{t} + \frac{\bar{r}}{\bar{r}^2+a^2}\left(\bar{x}d\bar{x} + \bar{y}d\bar{y}\right) + \frac{a(\bar{y}d\bar{x} - \bar{x}d\bar{y})}{\bar{r}^2+a^2} + \frac{\bar{z}d\bar{z}}{\bar{r}}\right]^2 \quad (11)$$

where we rewrote the Kerr metric in the second line in a form that will be useful in the following. In the $a \to 0$ limit, we recover the Schwarzschild metric in Kerr-Schild coordinates. The radial coordinate $\bar{r}$ is related to the fundamental coordinates $\bar{x}, \bar{y}, \bar{z}$ by the equation of an oblate ellipsoid

$$\frac{\bar{x}^2 + \bar{y}^2}{\bar{r}^2 + a^2} + \frac{\bar{z}^2}{\bar{r}^2} = 1 \quad (12)$$

which is equivalent to a quadratic equation in $\bar{r}^2$

$$\bar{r}^4 - \bar{r}^2(\bar{x}^2 + \bar{y}^2 + \bar{z}^2 - a^2) - a^2\bar{z}^2 = 0\,, \quad (13)$$

and the horizon is located at $\bar{r} = r_+ = M + \sqrt{M^2 - a^2}$. Eq. (12) motivates spheroidal coordinates:

$$\begin{aligned} \bar{x} &= \sqrt{\bar{r}^2 + a^2}\sin\bar{\theta}\cos\bar{\phi} \\ \bar{y} &= \sqrt{\bar{r}^2 + a^2}\sin\bar{\theta}\sin\bar{\phi} \\ \bar{z} &= \bar{r}\cos\bar{\theta}. \end{aligned} \quad (14)$$

We now explicitly reintroduce the cylindrical coordinates $(\bar{r}_{||}, \bar{r}_\perp, \bar{\phi}_{cyl})$ of the previous section :

$$\begin{aligned} \bar{x} &= \bar{r}_{||}\sin\theta_\beta\cos\phi_\beta + \bar{r}_\perp\left(\cos\theta_\beta\cos\phi_\beta\cos\bar{\phi}_{cyl} - \sin\phi_\beta\sin\bar{\phi}_{cyl}\right) \\ \bar{y} &= \bar{r}_{||}\sin\theta_\beta\sin\phi_\beta + \bar{r}_\perp\left(\cos\theta_\beta\sin\phi_\beta\cos\bar{\phi}_{cyl} + \cos\phi_\beta\sin\bar{\phi}_{cyl}\right) \\ \bar{z} &= \bar{r}_{||}\cos\theta_\beta - \bar{r}_\perp\sin\theta_\beta\cos\bar{\phi}_{cyl} \end{aligned} \quad (15)$$

The angles θ_β, ϕ_β specify the direction of the Lorentz boost β in spherical coordinates based on $\bar{x}, \bar{y}, \bar{z}$: $\beta = (\beta\sin\theta_\beta\cos\phi_\beta, \beta\sin\theta_\beta\sin\phi_\beta, \beta\cos\theta_\beta)$. With the coordinate transformation in Eq. (15) the Kerr metric becomes

$$\begin{aligned} ds^2 \quad = \quad & -d\bar{t}^2 + d\bar{r}_{||}^2 + d\bar{r}_\perp^2 + \bar{r}_\perp^2 d\bar{\phi}_{cyl}^2 \\ & + \frac{2M\bar{r}}{\bar{r}^4 + a^2\left(\bar{r}_{||}\cos\theta_\beta - \bar{r}_\perp\sin\theta_\beta\cos\bar{\phi}_{cyl}\right)^2} \\ & \times \left[d\bar{t} + \frac{\bar{r}}{\bar{r}^2+a^2}\left(\bar{x}d\bar{x} + \bar{y}d\bar{y}\right) + \frac{\bar{z}d\bar{z}}{\bar{r}} + \frac{a\left(\sin\theta_\beta\left[\bar{r}_\perp d\bar{r}_{||} - \bar{r}_{||}\,d(\bar{r}_\perp\sin\bar{\phi}_{cyl})\right] - \cos\theta_\beta\bar{r}_\perp^2 d\bar{\phi}_{cyl}\right)}{\bar{r}^2+a^2}\right]^2 \end{aligned} \quad (16)$$

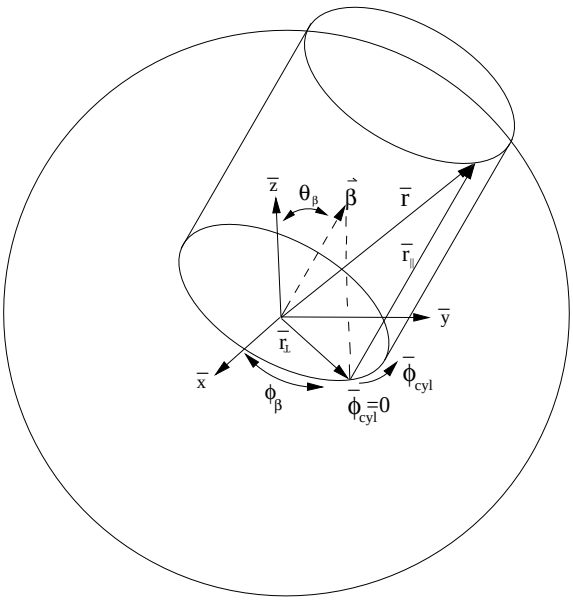


FIG. 3: The tilted cylindrical coordinates $(\bar{r}_{||}, \bar{r}_{\perp}, \bar{\phi}_{cyl})$ along with the radial coordinate r and Kerr-Schild Cartesian coordinates $(\bar{x}, \bar{y}, \bar{z})$. The vector β points along the boost direction, which is parallel to the symmetry axis of the cylinder.

We now carry out a boost along the selected cylindrical axis. Unbarred coordinates will denote the boosted observer frame. They are related to the barred rest-frame coordinates via Eq. (4). After boosting this metric, we will look at it on an arbitrary $t = constant$ hypersurface, which we take as $t = 0$ since this choice simplifies the expressions, to project out the spatial geometry of the hypersurface in which the apparent horizon lies. This will leave us with $d\bar{t} = -\gamma\beta dr_{||}$ and $\bar{r}_{||} = \gamma r_{||}$. With these changes substituted into Eq. (16) we obtain the spatial part of the boosted Kerr metric on a $t = 0$ hypersurface:

$$\begin{aligned} ds^2|_{t=0} &= dr_{||}^2 + dr_{\perp}^2 + r_{\perp}^2 d\phi_{cyl}^2 \\ &+ \frac{2M\bar{r}}{\bar{r}^4 + a^2\left(\gamma r_{||}\cos\theta_{\beta} - r_{\perp}\sin\theta_{\beta}\cos\phi_{cyl}\right)^2} \end{aligned}$$

$$\times \left[-\gamma\beta dr_{||} + \frac{\bar{r}}{\bar{r}^2+a^2}\left(\bar{x}d\bar{x}+\bar{y}d\bar{y}\right) + \frac{\bar{z}d\bar{z}}{\bar{r}} + \frac{a\left(\sin\theta_\beta\gamma\left[r_\perp dr_{||} - r_{||}\, d(r_\perp \sin\phi_{cyl})\right] - \cos\theta_\beta r_\perp^2 d\phi\right.}{\bar{r}^2+a^2}\right.$$

where a few terms involving $\bar{x}\,,\bar{y}\,,\bar{z}\,,\bar{r}$ in Eqs. (16), (17) were left untouched with the next step in mind. If one wishes, one could also write all of these terms as functions of $r_{||}, r_\perp$ and ϕ_{cyl}.

Let us remember what we are after; the 2-metric of the boosted geometry projected out by the condition $\bar{r} = r_+$. Eq. (12) implies

$$\frac{\bar{x}d\bar{x}+\bar{y}d\bar{y}}{\bar{r}^2+a^2} + \frac{\bar{z}d\bar{z}}{\bar{r}^2} = \left(\frac{\bar{x}^2+\bar{y}^2}{\left(\bar{r}^2+a^2\right)^2} + \frac{\bar{z}^2}{\bar{r}^4}\right)\bar{r}d\bar{r} \;\longrightarrow 0 \quad \text{at} \quad \bar{r} = r_+\,. \tag{18}$$

Thus if $d\bar{r} = 0$ (e.g. on the horizon, $\bar{r} = r_+$), the left hand side of Eq. (18) vanishes. This is the analogue of Eq. (6) for the Schwarzschild case of Section I. This simplification reduces the complexities of Eq. (17) substantially:

$$ds^2|_{t=0,\,\bar{r}=r_+} = \left[\begin{array}{l} dr_{||}^2 + dr_\perp^2 + r_\perp^2 d\phi_{cyl}^2 + \frac{2Mr_+}{r_+^4+a^2\left(\gamma r_{||}\cos\theta_\beta - r_\perp\sin\theta_\beta\cos\phi_{cyl}\right)^2} \\ \qquad \times\left[-\gamma\beta dr_{||} + \frac{a\left(\sin\theta_\beta\gamma\left[r_\perp dr_{||} - r_{||}\,d(r_\perp\sin\phi_{cyl})\right] - \cos\theta_\beta r_\perp^2 d\phi_{cyl}\right)}{r_+^2+a^2}\right]^2 \end{array}\right]_{\bar{r}=r_+} . \tag{19}$$

However, it is difficult to translate the horizon condition $\bar{r} = r_+$ into something meaningful in cylindrical coordinates. Therefore, we must rewrite Eq. (19) in spheroidal coordinates to impose the condition $\bar{r} = r_+$ to extract the 2-metric of the apparent horizon. We do this by going back to Eqs. (15) and rewriting them as a matrix equation for both boosted and unboosted coordinates

$$\begin{pmatrix} \bar{x} \\ \bar{y} \\ \bar{z} \end{pmatrix} = \hat{M}\begin{pmatrix} \bar{r}_\perp\cos\bar{\phi}_{cyl} \\ \bar{r}_\perp\sin\bar{\phi}_{cyl} \\ \bar{r}_{||} \end{pmatrix} = \hat{M}\begin{pmatrix} r_\perp\cos\phi_{cyl} \\ r_\perp\sin\phi_{cyl} \\ \gamma r_{||} \end{pmatrix} \tag{20}$$

where the components of the matrix $\hat{M}$ can be determined from Eqs. (15). The radial coordinate $\bar{r}$ in Eq. (14) is related to the Cartesian and cylindrical coordinates via $\bar{x}^2 + \bar{y}^2 + \bar{z}^2 = \bar{r}_\perp^2 + \bar{r}_{||}^2 = \bar{r}^2 + a^2\sin^2\bar{\theta}$. Since $\bar{r}_{||} = \gamma r_{||}$ on the $t = 0$ hypersurface, we also have $r_\perp^2 + \gamma^2 r_{||}^2 = \bar{r}^2 + a^2\sin^2\bar{\theta}$ (cf. [8]). Setting Eq. (20) equal to Eq. (14) and multiplying by $\hat{M}^{-1}$, we get

$$\begin{pmatrix} r_\perp\cos\phi_{cyl} \\ r_\perp\sin\phi_{cyl} \\ \gamma r_{||} \end{pmatrix} = \hat{M}^{-1}\begin{pmatrix} \sqrt{\bar{r}^2+a^2}\sin\bar{\theta}\cos\bar{\phi} \\ \sqrt{\bar{r}^2+a^2}\sin\bar{\theta}\sin\bar{\phi} \\ \bar{r}\cos\bar{\theta} \end{pmatrix}.$$

Expanding this we obtain

$$\begin{aligned} r_\perp \cos\phi_{cyl} &= \cos\theta_\beta \cos\phi_\beta \sqrt{\bar{r}^2+a^2}\sin\bar{\theta}\cos\bar{\phi} + \cos\theta_\beta \sin\phi_\beta \sqrt{\bar{r}^2+a^2}\sin\bar{\theta}\sin\bar{\phi} - \sin\theta_\beta\ \bar{r}\cos\bar{\theta} \\ r_\perp \sin\phi_{cyl} &= -\sin\phi_\beta \sqrt{\bar{r}^2+a^2}\sin\bar{\theta}\cos\bar{\phi} + \cos\phi_\beta \sqrt{\bar{r}^2+a^2}\sin\bar{\theta}\sin\bar{\phi} \\ \gamma r_{||} &= \sin\theta_\beta \cos\phi_\beta \sqrt{\bar{r}^2+a^2}\sin\bar{\theta}\cos\bar{\phi} + \sin\theta_\beta \sin\phi_\beta \sqrt{\bar{r}^2+a^2}\sin\bar{\theta}\sin\bar{\phi} + \cos\theta_\beta\ \bar{r}\cos\bar{\theta}\,. \end{aligned} \tag{21}$$

In the limit $\theta_\beta = \phi_\beta = 0$, the equations above reduce to Eq. (14) with the cylindrical coordinates replacing $(\bar{x}, \bar{y}, \bar{z})$. This is the case of boosting along the z-axis, and we briefly treat that here before proceeding. For boost along the z-axis, with $\bar{r} = r_+$ (i.e. on the horizon) we have

$$ds^2|_{t=0,\,\bar{r}=r_+} = \left[dx^2 + dy^2 + dz^2 + \frac{r_+^2\,(r_+^2+a^2)}{r_+^4+\gamma^2 a^2 z^2}\left[-\gamma\beta dz + \frac{a(ydx - xdy)}{r_+^2+a^2}\right]^2 \right]_{\bar{r}=r_+} . \tag{22}$$

Because of the boost in the z-direction, only the terms involving z ($-\gamma\beta dz$ in the numerator and $\gamma^2 a^2 z^2$ in the denominator) differ from the unboosted case. In Eq. (22) we still have to evaluate some of the terms at $\bar{r} = r_+$. Using spheroidal coordinates

$$\begin{aligned} x &= \sqrt{r_+^2+a^2}\sin\bar{\theta}\cos\bar{\phi} \\ y &= \sqrt{r_+^2+a^2}\sin\bar{\theta}\sin\bar{\phi} \\ \gamma z &= r_+\cos\bar{\theta} \end{aligned} \tag{23}$$

we get

$$\begin{aligned} ds^2|_{t=0,\,\bar{r}=r_+} &= (r_+^2+a^2)(\cos^2\bar{\theta}d\bar{\theta}^2 + \sin^2\bar{\theta}d\bar{\phi}^2) + \frac{r_+^2}{\gamma^2}\sin^2\bar{\theta}d\bar{\theta}^2 \\ &+ \frac{r_+^2+a^2}{r_+^2+a^2\cos^2\bar{\theta}}\left[\beta r_+ \sin\bar{\theta}d\bar{\theta} - a\sin^2\bar{\theta}d\bar{\phi}\right]^2 . \end{aligned} \tag{24}$$

With further simplifications, this becomes

$$ds^2|_{t=0,\,\bar{r}=r_+} = (r_+^2 + a^2\cos^2\bar{\theta})d\bar{\theta}^2 + \frac{\sin^2\bar{\theta}}{r_+^2+a^2\cos^2\bar{\theta}}\left[-\beta a r_+ \sin\bar{\theta}d\bar{\theta} + (r_+^2+a^2)d\bar{\phi}\right]^2 . \tag{25}$$

In the $a \to 0$ limit, Eq. (25) gives precisely the expression we obtained for the boosted Schwarzschild metric. Let us now look at the 2-metric $g_{AB}(A, B = \theta, \phi)$ for the apparent horizon component by component.

$$g_{\bar{\theta}\bar{\theta}} = \left(r_+^2 + a^2\cos^2\bar{\theta}\right) + \left(\frac{\gamma\beta a r_+ \sin^2\bar{\theta}}{\sqrt{r_+^2+a^2\cos^2\bar{\theta}}}\right)^2 ,$$

$$g_{\bar{\phi}\bar{\phi}} = \left(\frac{(r_+^2 + a^2)\sin\bar{\theta}}{\sqrt{r_+^2 + a^2\cos^2\bar{\theta}}} \right)^2 ,$$
$$g_{\bar{\theta}\bar{\phi}} = -\left(\frac{(r_+^2 + a^2)\sin\bar{\theta}}{\sqrt{r_+^2 + a^2\cos^2\bar{\theta}}} \right) \left(\frac{\gamma\beta a r_+ \sin^2\bar{\theta}}{\sqrt{r_+^2 + a^2\cos^2\bar{\theta}}} \right) . \quad (26)$$

For any 2×2 matrix of the form

$$H_{AB} = \begin{pmatrix} A^2 + B^2 & BC \\ BC & C^2 \end{pmatrix} \quad (27)$$

the determinant is $detH_{AB} = A^2C^2$. The 2-dimensional metric is of this form, so

$$\sqrt{det\,(g_{AB})} = (r_+^2 + a^2)\sin\bar{\theta} \quad (28)$$

Since

$$\text{Area} = \int \sqrt{det\,(g_{AB})} d\bar{\theta} d\bar{\phi} \quad (29)$$

we obtain an area of $4\pi\left(r_+^2 + a^2\right)$ as expected, identical to the unboosted horizon area.

Going back to our boost in an arbitrary direction, we rewrite the 3-metric in Eq. (19) using the spheroidal coordinates of Eq. (21). After some algebra using a well known algebraic relation for the Kerr spacetime ($2Mr_+ = r_+^2 + a^2$) to simplify, and setting $\bar{r} = r_+$ in most places, we end up with a result surprisingly similar to Eq. (25)

$$ds^2|_{t=0,\bar{r}=r_+} = \left(r_+^2 + a^2 cos^2\bar{\theta}\right) d\bar{\theta}^2 + \frac{\sin^2\bar{\theta}}{r_+^2 + a^2\cos^2\bar{\theta}} \left[a\gamma\beta dr_{||} + \left(r_+^2 + a^2\right) d\bar{\phi}\right]^2 \quad (30)$$

Using the last one of Eqs. (21), we now expand the terms containing $dr_{||}$ and obtain the components of the 2-metric for the apparent horizon:

$$g_{\bar{\theta}\bar{\theta}} = \left(r_+^2 + a^2\cos^2\bar{\theta}\right) + \frac{\beta^2 a^2 \sin^2\bar{\theta}}{r_+^2 + a^2\cos^2\bar{\theta}} \left(\sqrt{r_+^2 + a^2}\sin\theta_\beta\cos\bar{\theta}\cos(\bar{\phi} - \phi_\beta) - r_+\cos\theta_\beta\sin\bar{\theta} \right)^2 , \quad (31)$$

$$g_{\bar{\phi}\bar{\phi}} = \frac{\left(r_+^2 + a^2\right)\sin^2\bar{\theta}}{r_+^2 + a^2\cos^2\bar{\theta}} \left(\sqrt{r_+^2 + a^2} - \beta a \sin\theta_\beta \sin\bar{\theta}\sin(\bar{\phi} - \phi_\beta) \right)^2 , \quad (32)$$

$$g_{\bar{\theta}\bar{\phi}} = \frac{\beta a\sqrt{r_+^2 + a^2}\sin^2\bar{\theta}}{r_+^2 + a^2\cos^2\bar{\theta}} \left[\begin{array}{c} \left(\sqrt{r_+^2 + a^2}\sin\theta_\beta\cos\bar{\theta}\cos(\bar{\phi} - \phi_\beta) - r_+\cos\theta_\beta\sin\bar{\theta} \right) \\ \times \left(\sqrt{r_+^2 + a^2} - \beta a\sin\theta_\beta\sin\bar{\theta}\sin(\bar{\phi} - \phi_\beta) \right) \end{array} \right] . \quad (33)$$

The $\beta \to 0$ limit of equations (31) through (32) yields the standard 2-metric of the Kerr spacetime given in Boyer-Lindquist coordinates. The $a \to 0$ limit gives the standard Schwarzschild (spherical) 2-metric. The $\theta_\beta = 0$ limit yields the metric of Eq. (26). Eqs. (31)-(33) show that g_{AB} is again of the form of Eq. (27). Hence the square root of the determinant of the metric is

$$\sqrt{\det\left(g_{AB}\right)} = \left(r_+^2 + a^2\right)\sin\bar{\theta} - \beta a\sqrt{r_+^2 + a^2}\sin\theta_\beta \sin^2\bar{\theta}\sin\left(\bar{\phi} - \phi_\beta\right). \tag{34}$$

The first term above is the familiar contribution from the unboosted Kerr metric. To determine the area, we integrate the square root of the determinant of the 2-metric over the angular variables of the spheroidal coordinate system.

$$\begin{aligned} \text{Area} &= \int \sqrt{\det\left(g_{AB}\right)} d\bar{\theta} d\bar{\phi} \\ &= \int_0^{2\pi} d\bar{\phi} \int_0^{\pi} d\bar{\theta} \left[\left(r_+^2 + a^2\right)\sin\bar{\theta} - \beta a\sqrt{r_+^2 + a^2}\sin\theta_\beta \sin^2\bar{\theta}\sin\left(\bar{\phi} - \phi_\beta\right)\right] \\ &= 4\pi\left(r_+^2 + a^2\right) . \end{aligned} \tag{35}$$

Above, the second term disappears because of the $\bar{\phi}$ integral. Our calculation shows that the area of the apparent horizon of a Kerr black hole remains invariant under arbitrary Lorentz boosts, as expected.

IV. CONCLUSIONS

Our goal was to show that the area of the apparent horizons of Kerr black holes remain invariant under a particular redefinition of the $t = constant$ hypersurface (Lorentz boosts in arbitrary directions on the Kerr-Schild form). We introduced boost-parallel cylindrical coordinates. In this form, it is almost trivial to boost the spacetime metric. Once boosted, we looked at a $t = constant$ hypersurface to determine the three dimensional spatial portion of the boosted metric, and projected down to the 2-metric of the apparent horizon. We gave examples and validation of using these results based on computational initial data, to obtain binding energy results for nonspinning black holes boosted together or apart. The binding energy curves with different β values closely overlap and agree in the Newtonian limit; the slight deviation of the binding energy from the $1/r$ form can plausibly be explained by nonlinear corrections to the physical separation corresponding to a given coordinate separation. This is a subject of a post-Newtonian study in progress.

For the general direction boosted Kerr case the 2-metric of the apparent horizon has non-zero off-diagonal terms; however, when integrated over the angular variables, these contribute zero to the area, leaving us with the same result as the undisturbed Kerr case, namely $Area = 4\pi\left(r_+^2 + a^2\right)$.

We performed all of our calculations in one particular type of slicing of the spacetime, i.e. $t = constant$. There are infinitely many slicings of static and stationary spacetimes, including ones with no apparent horizon at all [29]. But if the $t = constant$ space contains an apparent horizon then the horizon area has the standard value. Black holes are very special objects indeed.

Acknowledgments

This work was supported by NSF grant PHY-0354842 and NASA grant NNG 04GL37G. Sarp Akcay would like to thank Cihan Akcay for his assistance with MATlab.

---

[1] C. DeWitt, B.S. DeWitt, "Black Holes: Proceedings of the 23rd Les Houches Summer School", Gordon and Breach, New York (1973).

[2] S.W. Hawking, G.F.R. Ellis, *Large Scale Structure of Space-Time* (Cambridge University Press, Cambridge, 1973).

[3] Binary Black Hole Grand Alliance, *Phys. Rev. Lett.* **80**, 2512-2516, (1998).

[4] R.P. Kerr, A. Schild, "A New Class of Vacuum Solutions of the Einstein Field Equations", in *Proceedings of the Galileo Galilei Centenary Meeting on General Relativity, Problems of Energy and Gravitational Waves*, ed. G. Barbera (1965).

[5] Mijan Firdous Huq, "Apparent Horizon Location in Numerical Spacetimes" Ph.D. Thesis, The University of Texas at Austin, (2004).

[6] R. Matzner, M. F. Huq and D. Shoemaker, *Phys. Rev.* **D59**, 024015, (1999)[arXiv:gr-qc/9805023].

[7] M. F. Huq, M. Choptuik and R. A. Matzner, *Phys. Rev.* **D66**, 084024, (2002). [arXiv:gr-qc/0002076].

[8] E. Poisson, *A Relativist's Toolkit* (Cambridge University Press, Cambridge, 2004).

[9] C. W. Misner, K. S. Thorne, and J. A. Wheeler, *Gravitation* (W.H. Freeman, New York, 1970).

[10] M.P. Hobson, G. Efstathiou, and A.N. Lasenby, *General Relativity* (Cambridge University Press, Cambridge, 2006).

[11] S. Chandrasekhar, *The Mathematical Theory of Black Holes* (Oxford University Press, Oxford, 1983).

[12] F. Pretorius, *Phys. Rev. Lett.* **95**, 121101, (2005) [arXiv:gr-qc/0507014].

[13] J.G. Baker, J. Centrella, D. I. Choi, M. Koppitz and J. van Meter, *Phys. Rev. Lett.* **96**, 111102, (2006) [arXiv:gr-qc/0511103].

[14] M. Campanelli, C. O. Lousto, P. Marronetti and Y. Zlochower, *Phys. Rev. Lett.* **96**, 111101, (2006) [arXiv:gr-qc/0511048].

[15] J. A. Gonzalez, M. D. Hannam, U. Sperhake, B. Brugmann and S. Husa, arXiv:gr-qc/0702052, (2007).

[16] M. Campanelli, C. O. Lousto, Y. Zlochower and D. Merritt, *Phys. Rev. Lett.* **98**, 231102, (2007) [arXiv:gr-qc/0702133].

[17] B. Brugmann, J. A. Gonzalez, M. Hannam, S. Husa and U. Sperhake, arXiv:0707.0135, (2007).

[18] S. Brandt, B. Brügmann, *Phys. Rev. Lett.* **78**, 3606, (1997).

[19] R. A. Matzner, M. J. Huq, D. Shoemaker, *Phys. Rev.* **D59**, 024015, (1998).

[20] R. A. Matzner, A. Nerozzi, P. Walter, "openGR", 2008, in preparation.

[21] E. Bonning, P. Marronetti, D. Neilsen, R. A. Matzner, *Phys. Rev.* **D68**, 044019, (2003).

[22] S. Hawley, M. Vitalo, R. A. Matzner, arXiv:gr-qc/0604100, (2006).

[23] R. Genzel, R. Schödel, T. Ott, A. Eckart, T. Alexander, F. Lacombe, D. Rouan and B. Aschenbach, *Nature* **425**, 934, (2003).

[24] R. Shafee, J. E. McClintock, R. Narayan, S. W. Davis, L. Li, R. A. Remillard, *The Astrophysical Journal* **636**, L113, (2006).

[25] A. Broderick, V. L. Fish, S. S. Doeleman, A. Loeb, arXiv.org: 0809.4490, (2008).

[26] R. Matzner, "Area of the Apparent Horizon for a Schwarzschild Black Hole is Invariant under Lorentz Boosts in the z-direction." unpublished, (1996).

[27] R.E. Wald, *General Relativity* (The University of Chicago Press, Chicago, 1984).

[28] R. Arnowitt, S. Deser, and C. Misner, *Gravitation, an Introduction to Current Research* (Wiley, New York 1962).

[29] R.E. Wald, V. Iyer, *Phys. Rev.* **D44**, 3719, (1991).